Representation and Annual to Decadal Predictability of Euro-Atlantic Weather Regimes in the CMIP6 Version of the EC-Earth Coupled Climate Model

C. Delgado-Torres, D. Verfaillie, E. Mohino, M. Donat

JGR Atmospheres

RESEARCH ARTICLE
10.1029/2022JD036673

Key Points:

- The EC-Earth3 model simulates the spatial patterns and climatological frequencies of the Euro-Atlantic weather regimes realistically
- Correlations between simulated and observed frequencies of weather regimes on inter-annual to decadal time scales are generally low
- Model initialization does not significantly alter the skill in predicting the spatial patterns and temporal variations of the weather regimes

Supporting Information:

Supporting Information may be found in the online version of this article.

Correspondence to:

C. Delgado-Torres,
carlos.delgado@bsc.es

Citation:

Delgado-Torres, C., Verfaillie, D., Mohino, E., & Donat, M. G. (2022). Representation and annual to decadal predictability of Euro-Atlantic weather regimes in the CMIP6 version of the EC-Earth coupled climate model. *Journal of Geophysical Research: Atmospheres*, *127*, e2022JD036673. https://doi.org/10.1029/2022JD036673

Received 23 FEB 2022
Accepted 5 JUL 2022

Representation and Annual to Decadal Predictability of Euro-Atlantic Weather Regimes in the CMIP6 Version of the EC-Earth Coupled Climate Model

C. Delgado-Torres[1,2], D. Verfaillie[1,3], E. Mohino[2], and M. G. Donat[1,4]

[1]Barcelona Supercomputing Center (BSC), Barcelona, Spain, [2]Department of Physics of the Earth and Astrophysics, Universidad Complutense de Madrid, Madrid, Spain, [3]Aix-Marseille University, CNRS, IRD, Collège de France, INRAE, CEREGE, Aix-en-Provence, France, [4]Institució Catalana de Recerca i Estudis Avançats (ICREA), Barcelona, Spain

Abstract Weather regimes are large-scale atmospheric circulation states that frequently occur in the climate system with persistence and recurrence, and are associated with the occurrence of specific local weather conditions. This study evaluates the representation of the four Euro-Atlantic weather regimes in uninitialized historical forcing simulations and initialized decadal predictions performed with the EC-Earth3 coupled climate model. The four weather regimes are the positive and negative phases of the North Atlantic Oscillation (NAO+ and NAO−, respectively), Blocking, and Atlantic Ridge in winter; and the NAO−, Blocking, Atlantic Ridge, and Atlantic Low in summer. We also analyze the impact that the model initialization toward the observed state of the climate system has on the ability to predict the variability of the weather regimes' seasonal frequency of occurrence. We find that the EC-Earth3 model correctly reproduces the spatial patterns and climatological occurrence frequencies of the four weather regimes. By contrast, the skill in predicting the inter-annual to decadal variations of the weather regimes' seasonal frequencies is generally low, and the initialization does not significantly improve such skill. The observed teleconnections between the weather regimes and the North Atlantic sea surface temperatures are generally not reproduced by the model, which could be a reason for the low skill in predicting the temporal variations of the weather regime frequencies.

1. Introduction

Weather regimes are a set of climate states that occur more frequently due to either more persistence or more recurrence than other possible states of the climate system (Christensen et al., 2013; Cortesi et al., 2019; Michelangeli et al., 1995). They provide a simplified description of the atmospheric flow variability and describe large-scale conditions that can be associated with local weather. Skillful climate predictions of the weather regimes could thus be used as a source of predictability for local climate conditions (Hertig & Jacobeit, 2014). Therefore, a correct representation and prediction of weather regimes by climate models could be translated into useful climate information for decision-makers. At inter-annual to decadal time scales, such climate information could be provided by decadal climate predictions, which aim at filling the gap between seasonal predictions and climate projections (Kirtman et al., 2013).

The atmospheric states gather naturally into four well-defined, statistically robust clusters over the Euro-Atlantic sector, with a typical persistence of 3–7 days (Michelangeli et al., 1995). The four weather regimes are different across the seasons. In winter, the positive and negative phases of the North Atlantic Oscillation (NAO+ and NAO−, respectively), the Blocking, and the Atlantic Ridge are identified in the literature (Cattiaux, Quesada, et al., 2013; Cortesi et al., 2019, 2021; Dawson et al., 2012; Ferranti et al., 2015). In summer, the Euro-Atlantic weather regimes are the Atlantic Low, the NAO−, the Blocking, and the Atlantic Ridge (Cassou et al., 2005; Cattiaux, Quesada, et al., 2013). However, the existence and the optimal number of regimes is a subject with conflicting results (see, e.g., Christiansen [2007] for a review), and some studies even reject the existence of weather regimes (Stephenson et al., 2004). Still, a classification of flow regimes can be useful to characterize large-scale weather conditions and to evaluate how climate models represent large-scale atmospheric flow.

The simulation and prediction of the Euro-Atlantic weather regimes by climate models are hindered by the characteristic biases that models tend to show in the representation of atmospheric flow over the Euro-Atlantic domain (Walz et al., 2018). In particular, evaluations of climate models have often found an underestimation of the occurrence frequency and persistence of blocking events (Cattiaux, Quesada, et al., 2013; D'Andrea

et al., 1998; Masato et al., 2013; Schiemann et al., 2017), related to an overestimation of zonal (westerly) flow regimes in Europe (Donat et al., 2010). This paper therefore provides a systematic evaluation of climatological characteristics of weather regimes in the latest version of the EC-Earth model.

Climate predictions have been shown to skillfully predict essential climate variables at sub-seasonal to seasonal (Mariotti et al., 2020) and inter-annual to decadal (Kushnir et al., 2019) time scales, which can be useful to underpin decision-making in a wide range of sectors (Merryfield et al., 2020). These climate predictions use, in addition to external forcings (which provide skill in climate projections), predictability provided by slow variations of different components of the climate system, especially the ocean, land surface, and sea ice (Meehl et al., 2009, 2021). In order to make use of these potential sources of predictability, climate models are used to compute the future evolution of the climate system by integrating them forward in time from a set of observation-based initial conditions, which is referred to as model initialization.

On the seasonal time scale, Cortesi et al. (2017) showed skill in reproducing the weather regimes' spatial patterns, climatological frequencies, persistences, and transitions probabilities during winter, spring, and summer with the ECMWF seasonal forecasting system S4 (Molteni et al., 2011). However, they found low skill in reproducing the monthly frequency variations of the weather regimes. Carvalho-Oliveira et al. (2022) assessed the representation of the summer spatial patterns of the weather regimes within the MPI-ESM-MR seasonal forecasting system (Giorgetta et al., 2013), finding that the Atlantic Ridge regime shows the highest agreement with the reanalysis, while the Atlantic Low regime shows the lowest agreement. On inter-annual to decadal time scales, while decadal predictions in particular of temperature are skillful in many regions due to external forcings, model initialization has also been shown to add prediction skill for several climate variables (Smith et al., 2019). Also, some selected characteristics of large-scale atmospheric flow have been found to be predictable. For instance, Athanasiadis et al. (2020) have shown decadal prediction skill for the High Latitude Blocking and the NAO index during winter. Significant skill in predicting the NAO index was also found by Smith et al. (2020) using a very large ensemble based on multiple models and applying post-processing techniques to overcome the signal-to-noise problem in climate models (Scaife & Smith, 2018). However, a systematic evaluation addressing the decadal prediction skill of the objectively identified Euro-Atlantic weather regimes in different seasons as well as the impact that the initialization has on the skill is, to our knowledge, still missing.

The aim of this paper is twofold. On the one hand, we evaluate the fidelity of the EC-Earth3 model in reproducing the climatological patterns and frequencies of the Euro-Atlantic weather regimes. On the other hand, we compare the weather regimes in initialized decadal predictions and transient historical forcing simulations to quantify the impact of the model initialization on the skill in predicting the variability of the weather regimes on inter-annual to decadal time scales.

2. Data

In this study, a ten-member ensemble of initialized decadal predictions (DCPP; Boer et al., 2016) and a ten-member ensemble of non-initialized historical simulations (HIST) performed with the version 3.3 of the EC-Earth model (Döscher et al., 2022) in the framework of the Coupled Model Intercomparison Project Phase 6 (CMIP6; Eyring et al., 2016) are used. The historical simulations are started from different states of a pre-industrial control run with forcing held fix to 1850 levels, and are forced by observed external forcings until 2014. The decadal predictions have been produced by initializing the EC-Earth3 model every year from 1960 in November using a full-field initialization technique, and provide predictions for the next 11 years (Bilbao et al., 2021).

Two different reanalyses are used as reference datasets to evaluate the skill of the decadal predictions and historical simulations in representing the spatial patterns and climatological frequencies, and in predicting the variations of the seasonal frequency of occurrence of the weather regimes. These reanalyses are the Japanese 55-year Reanalysis (JRA-55; Kobayashi et al., 2015) and the NCEP/NCAR Reanalysis 1 (NCEP1; Kalnay et al., 1996). The main reason for choosing the JRA-55 and the NCEP1 reanalyses is their temporal coverage matching that of the decadal predictions. The JRA-55 data set is often preferred over others like NCEP1 because of its higher spatial resolution, making this reanalysis suitable for weather regime classification (Cortesi et al., 2019). However, here we use both reanalyses to take into account the observational uncertainty and assess the robustness of the results to the choice of the reference data set. Stryhal and Huth (2017) made a comparison between five different reanalyses (in which both the JRA-55 and NCEP1 were included) for the classification of patterns in the Euro-Atlantic

area in winter. They found that there is very little difference between the daily pattern classification, especially in mid-latitudes of the Northern Hemisphere (less than 8% of days classified differently), where there is a dense coverage of high-quality observations.

3. Methods

We use daily fields of sea level pressure (from the reanalyses and EC-Earth3 simulations) to compute the weather regimes over the Euro-Atlantic region delimited between 27°–81°N and 85.5°W–45°E, as in Cortesi et al. (2019). Some studies used the geopotential height at 500 or 700 hPa instead to compute the weather regimes (Casola & Wallace, 2007; Kageyama et al., 1999). However, we use the sea level pressure because it is a variable less affected by global warming than the geopotential height (Cortesi et al., 2021; Torralba et al., 2021) and the clustering will thus be more accurate over the long period considered. The winter (defined as December-January-February; DJF) and summer (defined as June-July-August; JJA) weather regimes are obtained during the 1965–2014 period (50 years) for the reanalyses, the historical simulations and the decadal predictions. For the reanalyses and the historical simulations, seasonal averages and multi-annual averages of seasonal means are considered. In the case of the decadal predictions, the first five individual forecast winters and summers, and all their possible multi-year averages have been included in the assessment. In addition, the analysis also includes the winters and summers for the average of forecast years 1–10 to account for the full predicted decade. Since different forecast periods are assessed, different start dates have been selected in each case in order to always evaluate the predictions over the same calendar period (i.e., over the 1965–2014 period). The evaluation period starts in 1965 because forecast year 5 is the last forecast year evaluated individually (and 1965 is the forecast year 5 from the first initialization, i.e., start date November 1960), and the evaluation period ends in 2014 because the historical simulations are run until that year.

The simulated data have been interpolated onto the spatial grid of the reanalyses to obtain the spatial patterns of the weather regimes in the same grid resolution and evaluate their spatial representation. Also, the daily pressure fields have been converted into daily anomalies by subtracting the daily climatology. The daily climatology has been computed over the whole period and smoothed by applying a Locally Estimated Scatterplot Smoothing filter (LOESS; Cleveland & Devlin, 1988) with a smoothing span of 1 to remove the short-term variability and retain the seasonal cycle (Torralba, 2019).

In order to classify the daily anomaly maps and compute the weather regimes, the *k*-means clustering algorithm (Michelangeli et al., 1995; Philipp et al., 2010) has been applied independently for each season and, in case of the historical simulations and decadal predictions, also independently for each ensemble member. The *k*-means algorithm aims at arranging a set of daily maps within groups, called clusters, seeking the most steady states. The algorithm minimizes the sum of the squared distances from each map to the centroid of the clusters to which they belong, providing the common spatial patterns in the analyzed area. The anomalies are previously weighted by the cosine of the latitude to take into account the different sizes of the grid boxes in the region considered (Cortesi et al., 2019, 2021; Falkena et al., 2020).

The number of clusters k to generate has to be specified in advance. Fereday et al. (2008) assessed the optimal number of clusters and concluded that there is no objective choice for the number of clusters. For small k values, the full range of patterns is not correctly represented, while if a large k is chosen different clusters can look very similar. The number of clusters generated in this study is $k = 4$, typically used in the literature to assess the Euro-Atlantic weather regimes (Cassou et al., 2005; Cattiaux, Quesada, et al., 2013; Cortesi et al., 2019, 2021; Dawson et al., 2012; Ferranti et al., 2015; Hertig & Jacobeit, 2014). In addition, to confirm that the four weather regimes are obtained even if the *k*-means algorithm is set to define more clusters, the same procedure has been used but applying the *k*-means algorithm to identify five clusters ($k = 5$). Similarly, the first and second halves of the evaluation period (i.e., 1965–1989 and 1990–2014) have been used to obtain the four weather regimes ($k = 4$, as in the rest of the study) to confirm that such weather regimes are present during the whole period.

The observed and simulated weather regimes are independently computed by cluster analysis with the *k*-means algorithm applied to the daily anomalies fields to obtain the spatial patterns. Then, the daily maps are projected onto the four patterns using the minimum Euclidean distance method. Both minimal-correlation and minimal-persistence filters are applied to both observed and simulated projected daily maps to filter out the days that do not actually belong to any of the clusters. The minimal-correlation filter consists of de-classifying those

days with a spatial correlation (measured with the spatial Anomaly Correlation Coefficient, ACC; Wilks, 2011) lower than 0.25 with the cluster it was assigned. The minimal-persistence filter de-classifies those days that do not belong to a spell of at least 3 days. This methodology is similar to that used in Cattiaux, Douville, and Peings (2013) but without previously applying Empirical Orthogonal Functions to take into account the extreme sea level pressure values. This method tests whether the EC-Earth3 model correctly represents the weather regimes' spatial patterns by itself. Additionally, the same methodology has been employed but projecting the simulated daily maps onto the observed clusters (i.e., only applying the *k*-means algorithm to the reanalysis data) to assess how the simulated daily maps fit onto the observed patterns. Results in the main text correspond to the first approach, that is, projecting the simulated and observed fields onto the simulated and observed patterns, respectively. The results for the alternative method, that is, projecting the simulated fields onto the observed patterns, are included in Supporting Information S1.

Once each day is assigned to one of the four seasonal clusters (or to the unclassified cluster), the spatial patterns of the weather regimes are computed as the composites (averaged daily maps) of all the days that have been assigned to a cluster. The relative seasonal frequency of occurrence of each weather regime is computed as the percentage of the number of days per season assigned to each cluster. For the simulations, since the clustering has been applied to each ensemble member separately, the frequency time series and the spatial patterns are calculated as the ensemble mean.

The spatial correlation between the simulated and observed patterns is estimated with the spatial ACC. This metric has been computed by accounting for the different sizes of the grid cells. The significance of the spatial correlation has been assessed by estimating the confidence intervals at the 95% confidence level computed by a Fisher transformation. If the confidence interval includes zero, the spatial correlation is not significant. The spatial correlation difference between the historical simulations and decadal predictions is significant if their confidence intervals do not overlap. A two-sided Kolmogorov-Smirnov test has been applied to assess whether the simulated and observed distributions of the seasonal frequencies could have been sampled from the same continuous distribution at the 95% confidence level. In addition, a two-sided *t*-test has been used to assess whether the mean values of the simulated and observed distributions are statistically different at the 95% confidence level. In order to estimate the temporal correlation, the Pearson's correlation coefficient is used. A two-tailed *t*-test is applied to analyze whether the temporal correlation between experiments and reanalyses is statistically significant at the 95% confidence level. The Fisher's z transformed correlations divided by the standard error of the difference (Wilks, 2011) are used to assess whether the correlations obtained with the historical simulations and the decadal predictions are statistically different at the 95% confidence level. In order to avoid a potential overestimation of the statistical significance due to spatial patterns and time series autocorrelation, the effective degrees of freedom have been used for the significance tests. Such effective degrees of freedom have been calculated over the reanalysis data following Zwiers and von Storch (1995). In the case of the spatial patterns, the methodology has been applied over the vector created by concatenating all latitudes one after the other. It should be noted that part of the information related to different latitudes might be lost when computing the effective number of degrees of freedom for the spatial patterns.

4. Results

4.1. Evaluation of the Spatial Patterns and Climatological Frequencies of the Weather Regimes

We first evaluate two climatological aspects of weather regimes: the spatial patterns (i.e., the composites pressure maps of all the days that belong to each weather regime) and the climatological seasonal frequencies of occurrence.

The spatial patterns of the observed weather regimes during the winter and summer seasons identified in the JRA-55 reanalysis are shown in Figure 1. The four clusters obtained for each season correspond to the NAO+, NAO−, Blocking, and Atlantic Ridge during winter; and the Atlantic Low, NAO−, Blocking, and Atlantic Ridge during summer. The regime patterns show that the amplitude of the clusters' anomalies is higher during the winter season, when they are more persistent in time and have a stronger effect on local climate (Ferranti et al., 2015; Fil & Dubus, 2005). Compared with the spatial patterns using the NCEP1 reanalysis (Figure S1 in Supporting Information S1), there is a high consistency for both seasons, indicating the robustness of the identified weather regimes to the choice of the reference data set.

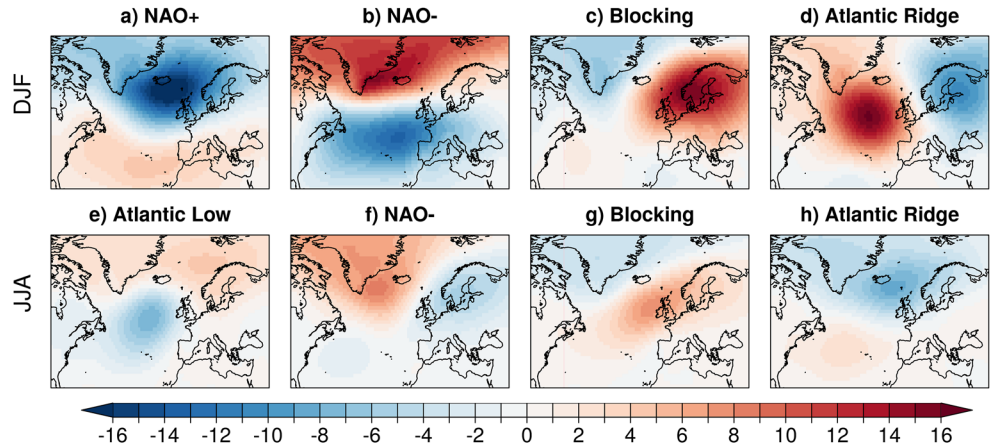

Figure 1. Spatial patterns of the observed Euro-Atlantic weather regimes (computed as the averaged sea level pressure anomalies, in hPa, of all the days classified onto each cluster) obtained with the JRA-55 reanalysis for winter and summer during the 1965–2014 period.

We test the sensitivity of the clustering algorithm results to the number of identified clusters and the period used to identify the clusters. We find that the same four observed weather regimes for winter are obtained when asking for five clusters (Figure S2 in Supporting Information S1). The additional cluster is represented as a center of anomalously negative pressure over the central part of the region considered. The sum of NAO+ and the additional cluster resembles the original NAO+ obtained with $k = 4$. When applying the k-means algorithm to the first and second halves of the evaluation period, both sets of clusters represent the same weather regimes as when using the whole period. However, some discrepancies are found in the first half (1965–1989) for NAO+ (for which the northern part of Europe contains a positive anomaly, while the anomalies over that region are slightly negative when using the whole period) and Blocking (which is displaced westward with respect to the original one). For summer (Figure S3 in Supporting Information S1), the patterns obtained with $k = 5$ and with different period halves are similar to the original ones.

The spatial patterns of the four weather regimes obtained during the whole period with both DCPP and HIST show a high agreement with the observed patterns in winter, being significant for all the forecast years and multi-year averages (Figure 2a). For summer, significant spatial correlations are also found for the NAO−, Blocking, and Atlantic Ridge regimes for both DCPP and HIST. However, the spatial correlations for DCPP are systematically high and significant for the Atlantic Low regime, except for the forecast years 1–2 (this exception is not found when using the NCEP1 reanalysis as the reference data set; Figure S4 in Supporting Information S1), while low and non-significant correlations are found for HIST. Furthermore, the spatial correlations for the different forecast years in the decadal predictions are similar for both seasons, indicating that the simulation of the weather regimes' patterns is not strongly affected by the climate drift in the decadal predictions. Similar results are found when using the NCEP1 reanalysis as the reference data set (Figure S4 in Supporting Information S1).

The ACC differences between DCPP and HIST are computed to assess whether the model initialization impacts the representation of the simulated weather regimes' patterns. The pattern correlation for the forecast periods that include more than one season is compared to the pattern correlation obtained with the historical simulations averaged over the same period length (e.g., the forecast years 1–3 are compared to 3-year averages from the historical simulations). The ACC differences (Figure 2b) indicate that DCPP and HIST perform equally in representing the spatial patterns of all weather regimes during winter, and the spatial patterns of the NAO−, Blocking and Atlantic Ridge regimes during summer (low ACC differences for all the cases, and only a few cases show significance). For the summer Atlantic Low regime, the results show an added value of model initialization in representing the spatial pattern of this weather regime. It should be noted that, even using the effective degrees of freedom to account for the auto-correlation, the sample size is still large, which means that relatively low ACC values and ACC differences may be significant.

The previous analysis (Figure 2) is focused on evaluating the agreement between the model-specific and observed spatial patterns. If, instead, we compare the observed patterns with the patterns obtained by projecting the

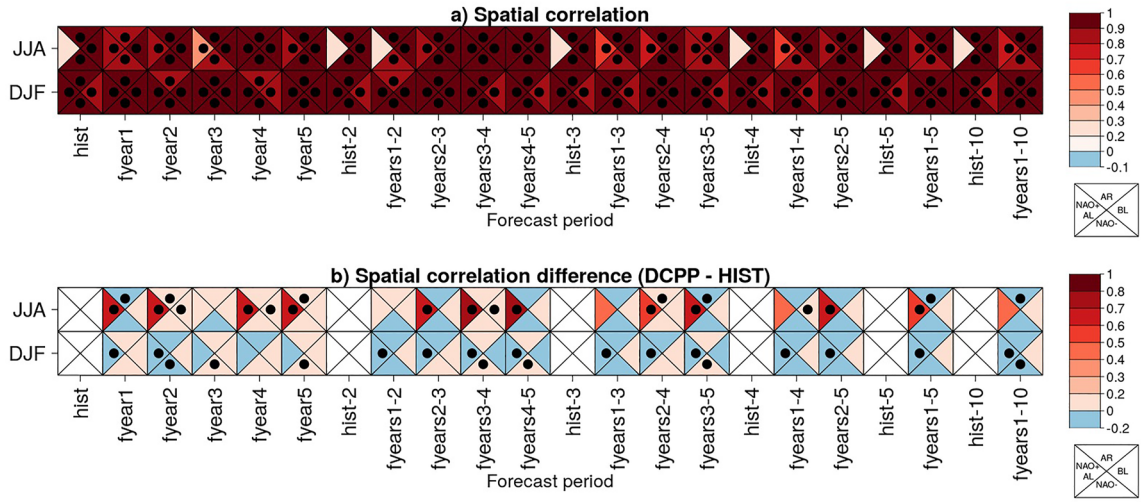

Figure 2. (a) Spatial correlation between the observed and simulated Euro-Atlantic weather regimes' patterns. (b) Difference between the ACC obtained with the decadal predictions and that obtained with the historical simulations. The evaluations period is 1965–2014. The reference data set is the JRA-55 reanalysis. The rows correspond to the winter and summer seasons. The different columns display the results for individual and multi-year averages, where hist-X corresponds to X-years averaged historical simulations and fyearsY-Z corresponds to decadal predictions for the forecast years Y-Z. Dots indicate that the correlation (a) or the correlation difference (b) is statistically significant at the 95% confidence level. The auto-correlation of the spatial patterns has been taken into account to determine the effective sample size when computing the statistical significance.

simulated daily maps onto the observed clusters (i.e., forcing the simulated daily maps to fit into the observed patterns), high and significant spatial correlations are obtained for all the weather regimes by definition. In addition, no differences between DCPP and HIST are found (Figure S5 in Supporting Information S1).

In the following, we evaluate the representation of the climatological frequency of occurrence. Figure 3 shows the distribution of the weather regimes' frequencies for the JRA-55 reanalysis, historical simulations, and decadal predictions for the first forecast year. The observed frequencies in winter show that the most frequent weather regime is NAO+ (with 23.3% of the days assigned to this cluster), followed by Blocking (20.6%), NAO− (19.1%), and Atlantic Ridge (18.1%). In summer, the most frequently observed weather regime is Blocking (21.2% of the days), followed by Atlantic Ridge (18.8%), Atlantic Low (17.8%), and NAO− (17.2%). Note that the weather regimes' frequencies do not add up to 100% due to the use of an unclassified cluster (see Section 3).

Both DCPP and HIST show a correct representation of the mean frequencies, which are found to not be significantly different to the observed mean frequencies by applying a *t*-test at the 95% confidence level. In addition, we

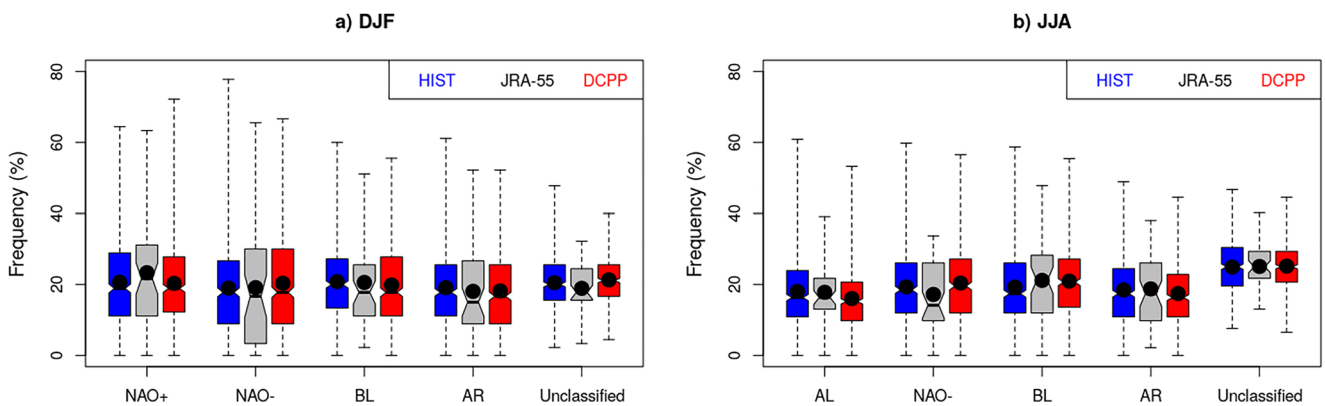

Figure 3. Box-and-whisker diagrams of the seasonal frequencies of occurrence for the Euro-Atlantic weather regimes and the unclassified cluster for winter (a) and summer (b) during the 1965–2014 period. The results are shown for the historical simulations (in blue), the JRA-55 reanalysis (in gray), and the decadal predictions (in red). Dots show the mean frequencies, while the whiskers indicate the data range between the minimum and maximum values. Model simulation boxes have been obtained using all ensemble members without averaging.

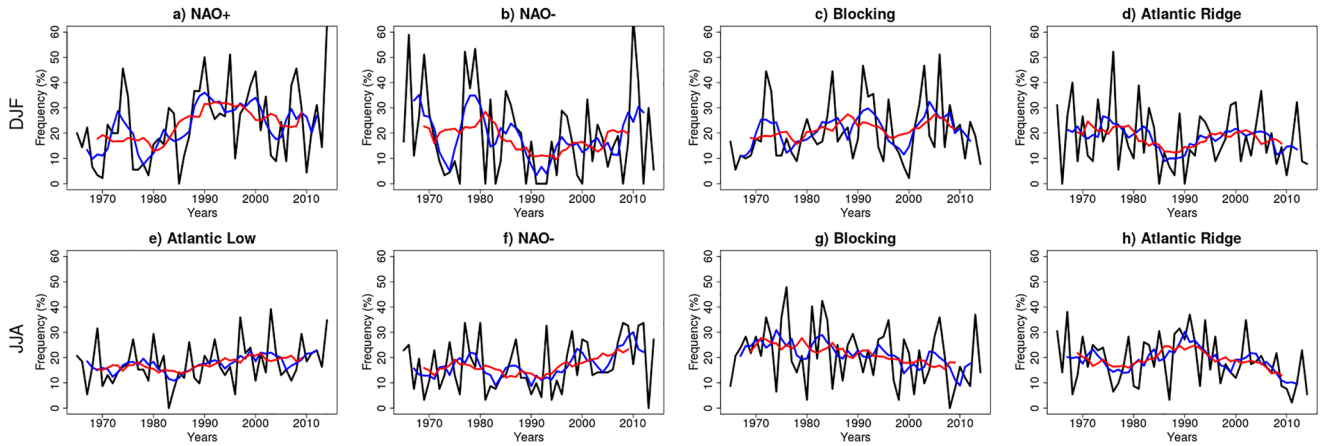

Figure 4. Time series of the weather regime frequencies of occurrence obtained with the JRA-55 reanalysis during winter (top row) and summer (bottom row) during the 1965–2014 period. In addition to 1-season averages (in black), also running averages over 5 (in blue) and 10 (in red) seasonal data points are shown.

assessed whether the simulated distributions are drawn from the same distribution as the observed ones with the Kolmogorov-Smirnov test. We find that the observed and simulated frequencies could have been drawn from the same continuous distribution, pointing to the correct representation of the frequency distribution by both DCPP and HIST. The same results are found when using the NCEP1 reanalysis as the reference data set (Figure S6 in Supporting Information S1).

The percentage of days that have been unclassified (due to either low spatial correlation or low persistence) is also shown in Figure 3. The results show that there are more unclassified days in summer than in winter, also found by Cattiaux, Douville, and Peings (2013). This happens for both the reanalyses and the climate model simulations. In the JRA-55 reanalysis, 18.9% of the days are unclassified in winter, while 25.1% of the days are unclassified during summer.

4.2. Annual to Decadal Prediction Skill of Weather Regime Frequencies

This section evaluates the skill in predicting the temporal variations of the weather regimes' seasonal occurrence frequencies (i.e., the percentage of the number of days assigned to each cluster). A skillful prediction of such variations may be useful for providing climate services based on weather regimes, which could potentially be used for downscaling the model output and as local climate predictors.

The time series obtained with the JRA-55 reanalysis show an inter-annual variability of the seasonal occurrence frequency of the weather regimes (i.e., the percentage of number of days assigned to each cluster) during both summer and winter (Figure 4). The 5-season and 10-season averages also show a temporal variability of the weather regimes' frequencies at multi-annual to decadal time scales. The time series obtained with the NCEP1 reanalysis show a similar variability as those obtained with JRA-55 (Figure S7 in Supporting Information S1). The time series show higher variability in winter than in summer at inter-annual to decadal time scales, particularly for the NAO+ and NAO− regimes. The NAO+ regime was found most frequently in the 1990s, when the NAO− was less frequent than in the previous and following decades, consistent with the time series of the NAO index shown, for example, by Athanasiadis et al. (2020) and Smith et al. (2020).

For prediction purposes, the phasing of the simulated variations of the weather regimes are compared against observations through time series correlation analysis. Figure 5a summarizes the correlation coefficients between the simulated (with both decadal predictions and historical simulations) and observed time series of the weather regimes.

In general, low correlation coefficients are found for both DCPP and HIST, with only a few cases being statistically significant. The temporal correlations for HIST mostly show coefficients close to zero. However, significantly positive correlations are found during winter for 2 and 3-year averages for the NAO− regime, and five and 10-year averages for the Atlantic Ridge regime. The correlation coefficients obtained for DCPP are generally

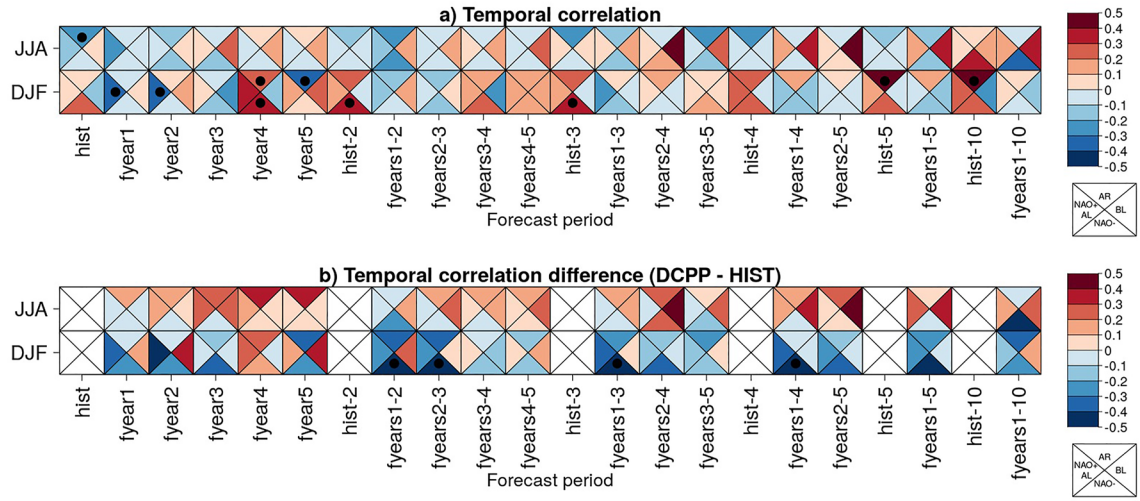

Figure 5. (a) Temporal correlation between the observed and simulated (for HIST and DCPP) Euro-Atlantic weather regimes' occurrence frequencies. (b) Difference between the correlation coefficient obtained with the decadal predictions and that obtained with the historical simulations. The evaluation period is 1965–2014. The rows correspond to the winter and summer seasons. The different columns display the results for individual and multi-year averages, where hist-X corresponds to X-years averaged historical simulations and fyearsY-Z corresponds to decadal predictions for the forecast years Y-Z. Dots indicate that the correlation (a) or the correlation difference (b) is statistically significant at the 95% confidence level. The auto-correlation of the time series has been taken into account to determine the effective sample size for the significance test.

low in winter and are significantly positive only for a few marginal cases (e.g., for NAO− and Atlantic Ridge for forecast year 4). For summer, the Blocking regime shows the highest correlation coefficients, especially when averaging at least four forecast years, but no significance is found.

In order to identify whether the model initialization has an impact on the predictability of the variability of weather regimes, the correlation differences between the decadal predictions and the historical simulations are calculated and displayed in Figure 5b. The figure does not show a clear pattern of the impact of initialization, and no significant improvements are found. In fact, the results show that the decadal predictions are less skillful in predicting the weather regimes' time series for some cases, especially for some multi-year averages of the NAO− regime during winter. The weather regime that tends to show some benefit from initialization (indicated by systematically positive correlation differences across different forecast times, although without significance) is the Blocking regime during summer. The Atlantic Ridge regime also shows an improvement from initialization (systematic for different forecast times, although not significant), but the temporal correlation is still negative for DCPP. Similar results are found when using NCEP1 as the reference data set (Figure S8 in Supporting Information S1).

4.3. Teleconnections Between the Weather Regimes and the North Atlantic SST

The slow variations of the SST provide predictability at decadal time scales (Doblas-Reyes et al., 2013; Rodwell et al., 1999; Sutton & Allen, 1997). Thus, the skill in predicting the North Atlantic SST may be transferred to some skill in predicting atmospheric circulation, as represented for example, by the Euro-Atlantic weather regimes. For this, it is needed that the model correctly reproduces (a) the observed variations of the North Atlantic SST and (b) the observed teleconnections between the weather regimes' frequencies and the North Atlantic SST.

For (a), Bilbao et al. (2021) performed a comprehensive assessment of the skill of the decadal predictions performed with the EC-Earth3 model. They showed that the model is skillful in predicting the SST over much of the North Atlantic but skill is poor in the central Subpolar North Atlantic region, and that the initialization leads to a decrease of the skill due to initialization shocks and the drift of the predictions. They discussed that these initialization issues over the North Atlantic may be improved by model development and by investigating better initialization strategies.

For (b), the observed and simulated correlations between the North Atlantic SST and the weather regime frequencies are analyzed (Figure 6). The observed teleconnection maps show that the frequencies of the weather regimes

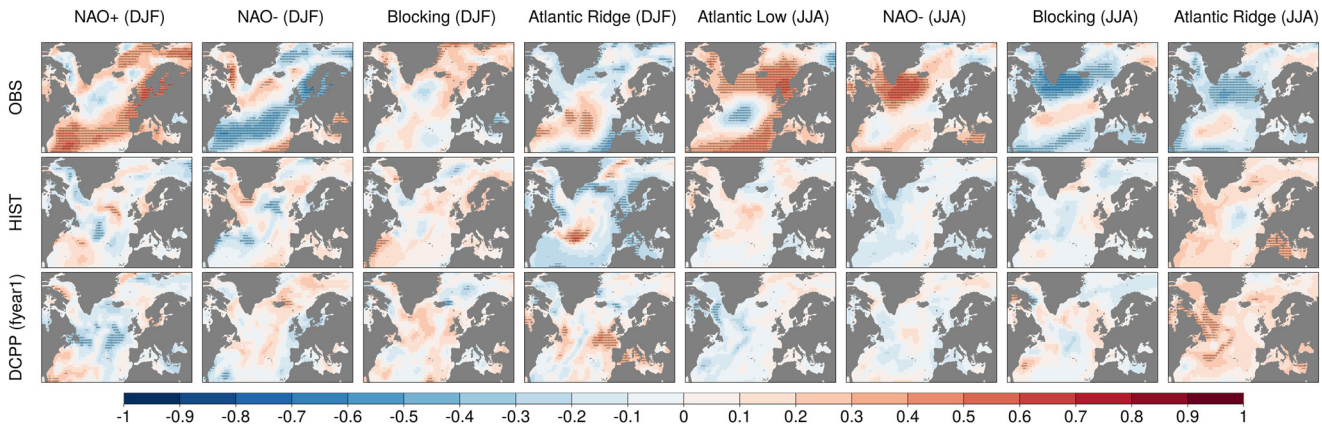

Figure 6. Correlation between the seasonal weather regimes frequency and the seasonal sea surface temperature for the JRA-55 reanalysis (top row), historical simulations (center row), and the first forecast year from decadal predictions (bottom row). In the case of the historical simulations and decadal predictions, the correlations have been computed with the ensemble mean. Dots indicate that the correlation is statistically significant at the 95% confidence level using a two-sided *t*-test. The time series' auto-correlation has been taken into account to determine the effective sample size for the significance test.

are significantly correlated with the SST over large areas of the North Atlantic Ocean, except for the winter Blocking regime which does not show significant correlations. However, this relationship is not correctly reproduced by the model, as the correlation maps show different patterns for both historical simulations and decadal predictions in comparison to that observed. Also, these teleconnections are weaker (in the sense that lower correlation coefficients are found) and in most cases not significant.

This could suggest that either (a) the weather regime frequency variations do not represent a predictable signal in relation to the SST and thus models have no possibility to predict it; (b) the relationship between the SST and weather regimes' frequency could be non-causal (SST anomalies do not force the weather regimes' frequency) and thus the phenomena phasing both are inherently unpredictable; (c) though inherently predictable, the low skill of EC-Earth3 in predicting the Subpolar North Atlantic SST (Bilbao et al., 2021) restricts the potential transferability of skill that may otherwise exist; or (d) the teleconnections are fundamentally predictable, but their signals are underestimated by the model and small compared to the noise in the ensemble.

5. Summary, Discussion, and Conclusions

This study evaluates the simulated weather regimes in the Euro-Atlantic sector in the EC-Earth3 coupled climate model in comparison to reanalyses data for the winter and summer seasons. The evaluation has been performed for both decadal predictions and historical simulations, and they are compared to assess the impact that the model initialization has on the skill.

We find that the EC-Earth3 model reproduces the spatial patterns of the four Euro-Atlantic weather regimes with high similarity to the observed patterns derived from the reanalyses. High spatial correlations are obtained with both decadal predictions and historical simulations except for the summer Atlantic Ridge regime, which shows spatial correlations close to zero for the historical simulations. Also, these spatial patterns are robust across different forecast years, indicating that they are not affected by the model drift in the decadal predictions.

Both the climatological mean frequencies and ranges of inter-annual variability in the occurrence frequencies of these weather regimes are well reproduced by the model. The number of unclassified days, due to either low spatial correlation with the observed pattern or low persistence of the regime event, is higher in summer (25.1%) than in winter (18.9%), which may be due to less intense pressure gradients during the summer season (Cattiaux, Douville, & Peings, 2013).

Regarding the skill in predicting the inter-annual and multi-annual variations of the occurrence frequencies of the weather regimes, low correlation coefficients are generally found to be, for the most part, not statistically significant. Exceptions are the winter NAO− and Atlantic Ridge regimes, which are found to be reproduced by the historical simulations with significant skill for multi-year averages. Although not statistically significant,

the decadal predictions tend to show a positive correlation with observations for the predictions of the Blocking regime during summer systematically at different forecast periods.

The comparison between the decadal predictions and the historical simulations indicates that the model initialization does not significantly improve the skill in predicting the weather regimes' variability. In fact, the skill decreases for some cases, especially for some multi-year averages of the NAO− regimes during winter. The highest potential benefit due to initialization is found for the Blocking regime during summer, with a systematic tendency toward positive ACC differences between DCPP and HIST across different forecast periods, but such differences are not statistically significant. The lack of added value due to initialization might be due to inconsistencies between the model and the initial conditions used to initialize the predictions (Bilbao et al., 2021). Better predictions of the variations of the Blocking regime's frequency could anticipate periods with more frequency of extreme events like cold air outbreaks, heat-waves, floods and droughts (Christensen et al., 2013), as well as episodes of high pollution over European regions (Garrido-Perez et al., 2017; Ordóñez et al., 2017).

While there is mounting evidence that climate models seem to underestimate some of the predictive signals related to atmospheric circulation, in particular in the Atlantic sector (Scaife & Smith, 2018; Smith et al., 2019), a few previous studies showed some predictability for selected weather types at multi-annual to decadal time scales. For example, Athanasiadis et al. (2020) showed decadal prediction skill for the High Latitude Blocking and the NAO index during the winter season using a large ensemble (40 members from the Community Earth System Model-Decadal Prediction Large Ensemble [CESM-DPLE; Yeager et al., 2018]). They showed that such a large ensemble allows the predictable component of the atmospheric variability to emerge from the chaotic noise. Smith et al. (2020) also showed predictability for the NAO index using a large multi-model ensemble from CMIP5 and CMIP6 models and applying post-processing techniques for overcoming the low signal-to-noise ratio of the raw model output. However, we use a different definition based on an objective weather regime classification designed to classify each day into a certain flow regime (or into the unclassified cluster).

In order to assess possible factors that limit the skill in predicting the weather regimes' frequencies, the observed and simulated teleconnections between the North Atlantic SST and the weather regime frequencies have been computed. The observed teleconnections show that the occurrence frequencies of the different weather regimes are significantly correlated with the SST over large regions of the North Atlantic Ocean (except for the winter Blocking regime, for which no significant correlations are found). However, these relationships are not shown in the teleconnections maps obtained with both the decadal predictions and historical simulations, limiting the skill that may potentially be transferred from the North Atlantic SST to the weather regimes' frequencies. Besides, the sea level pressure (variable used to compute the weather regimes) over the North Atlantic region particularly suffers from the signal-to-noise paradox (Smith et al., 2019), which may have contributed to reducing the skill in predicting the weather regimes. Previous studies have pointed to the benefits of using larger ensembles for predicting variables with a small predictive signal relative to the noise (Athanasiadis et al., 2020; Smith et al., 2020). In order to assess whether the results obtained with the relatively small ensemble size (10 ensemble members) can be improved using a larger ensemble, we have tested whether the skill improves when the ensemble size is doubled by including another 10 ensemble members with slightly different initialization but overall similar behavior (i.e., the skill is estimated with a total of 20 decadal prediction members), but the results are similar and no skill improvement is found (not shown). On the other hand, the low skill of the EC-Earth3 model in predicting the Subpolar North Atlantic SST shown by Bilbao et al. (2021) may also limit the skill that may potentially be transferred from the North Atlantic SST to the weather regimes' frequencies. The limitation of the skill in predicting the weather regimes' frequencies of occurrence due to biases in SSTs was also suggested by Fabiano et al. (2020). Another possible limitation might be the spatial resolution of the model. Recent works have shown that the representation of climatological frequencies and spatial patterns of some weather regimes (e.g., Blocking regime) can be improved by increasing the grid resolution of the atmospheric model (Dawson & Palmer, 2015; Fabiano et al., 2020). However, it is not clear if the increase in resolution can improve the prediction skill of the frequencies' variability.

In conclusion, this study demonstrates that the EC-Earth3 model, which is used for the contributions to CMIP6/DCPP-A, skillfully simulates most climatological aspects of Euro-Atlantic weather regimes. However, the skill in predicting the inter-annual to decadal variability of these weather regimes is low, and the model initialization does not significantly improve such skill (as seen by comparing the decadal predictions and historical simulations). This work can be the basis for more detailed future studies. For instance, further comparison with

other models could help answer the question of whether the lack of skill in the prediction of the weather regimes frequencies by the EC-Earth3 model is due to an inherently unpredictable signal or due to model deficiencies (since other models might be skillful in predicting the temporal variations of the weather regimes). On the other hand, the multi-model ensemble of predictions contributing to CMIP6/DCPP-A could be used to assess if the skill is improved compared to the individual models due to error compensation and to the signal that each model adds to the multi-model ensemble (Hagedorn et al., 2005). Also, post-processing techniques such as the calibration method proposed by Eade et al. (2014) or the post-processing and member selection as introduced by Smith et al. (2020) for NAO predictions could be implemented with the goal to improve the prediction of the objectively classified weather regimes. If the predictability of weather regimes can eventually be established robustly in the future, it could unlock the potential for skillful decadal climate predictions over Europe and the prediction of specific weather phenomena, including extreme events typically related to certain weather regimes.

Data Availability Statement

The EC-Earth3 decadal predictions (members r[1–10]i1p1f1; EC-Earth, 2019b) and historical simulations (members r[2,12,14,16–18,21-22,24–25]i1p1f1; EC-Earth, 2019a) are available for downloading on the ESGF node (https://esgf-node.llnl.gov/search/cmip6/). JRA-55 reanalysis data (Japan Meteorological Agency, Japan, 2013) have been retrieved from https://climatedataguide.ucar.edu/climate-data/jra-55. NCEP reanalysis data (National Centers for Environmental Prediction et al., 1994) have been retrieved from https://www.esrl.noaa.gov/psd/. The code used in this paper can be found at https://earth.bsc.es/gitlab/cdelgado/cdelgado_copernicus/-/tree/development_branch/WeatherRegimes/paper_i1. We acknowledge the use of the s2dv, startR, multiApply, CSTools (Pérez-Zanón et al., 2021), and ClimProjDiags R software packages, all of them available on CRAN (https://cran.r-project.org/).

Acknowledgments
This research has received support by the AXA Research Fund, the CLINSA project (CGL2017-85791-R), and the EUCP project (Horizon 2020 Grant 776613). CDT acknowledges financial support from the Spanish Ministry for Science and Innovation (FPI PRE2019-08864 financed by MCIN/AEI/10.13039/501100011033 and by FSE invierte en tu futuro). EH was supported by the Spanish Project PRE4CAST (grant CGL2017-86415-R). MGD has also been supported by the Spanish Ministry for the Economy, Industry and Competitiveness (grant RYC-2017-22964). The authors thank Verónica Torralba, Nicola Cortesi, Roberto Bilbao, Lluís Palma, and Francisco J. Doblas-Reyes for their technical and scientific support. The authors also thank the anonymous reviewers for their valuable comments and suggestions, which improved the manuscript.

References

Athanasiadis, P. J., Yeager, S., Kwon, Y. O., Bellucci, A., Smith, D. W., & Tibaldi, S. (2020). Decadal predictability of North Atlantic blocking and the NAO. *npj Climate and Atmospheric Science*, *3*(1), 20. https://doi.org/10.1038/s41612-020-0120-6

Bilbao, R., Wild, S., Ortega, P., Acosta-Navarro, J., Arsouze, T., Bretonnière, P. A., et al. (2021). Assessment of a full-field initialized decadal climate prediction system with the CMIP6 version of EC-Earth. *Earth System Dynamics*, *12*(1), 173–196. https://doi.org/10.5194/esd-12-173-2021

Boer, G. J., Smith, D. M., Cassou, C., Doblas-Reyes, F., Danabasoglu, G., Kirtman, B., et al. (2016). The Decadal Climate Prediction Project (DCPP) contribution to CMIP6. *Geoscientific Model Development*, *9*(10), 3751–3777. https://doi.org/10.5194/gmd-9-3751-2016

Carvalho-Oliveira, J., Borchert, L. F., Zorita, E., & Baehr, J. (2022). Self-organizing maps identify windows of opportunity for seasonal European summer predictions. *Frontiers in Climate*, *4*, 30. https://doi.org/10.3389/FCLIM.2022.844634/BIBTEX

Casola, J. H., & Wallace, J. M. (2007). Identifying weather regimes in the wintertime 500-hPa geopotential height field for the Pacific–North American sector using a limited-contour clustering technique. *Journal of Applied Meteorology and Climatology*, *46*(10), 1619–1630. https://doi.org/10.1175/JAM2564.1

Cassou, C., Terray, L., & Phillips, A. S. (2005). Tropical Atlantic influence on European heat waves. *Journal of Climate*, *18*(15), 2805–2811. https://doi.org/10.1175/JCLI3506.1

Cattiaux, J., Douville, H., & Peings, Y. (2013). European temperatures in CMIP5: Origins of present-day biases and future uncertainties. *Climate Dynamics*, *41*(11–12), 2889–2907. https://doi.org/10.1007/s00382-013-1731-y

Cattiaux, J., Quesada, B., Arakélian, A., Codron, F., Vautard, R., & Yiou, P. (2013). North-Atlantic dynamics and European temperature extremes in the IPSL model: Sensitivity to atmospheric resolution. *Climate Dynamics*, *40*(9–10), 2293–2310. https://doi.org/10.1007/s00382-012-1529-3

Christensen, J. H., Kanikicharla, K. K., Aldrian, E., An, S. I., Albuquerque Cavalcanti, I. F., de Castro, M., et al. (2013). *Climate phenomena and their relevance for future regional climate change*. In *Climate change 2013 the physical science basis: Working Group I Contribution to the Fifth Assessment Report of the Intergovernmental Panel on Climate Change*. https://doi.org/10.1017/CBO9781107415324.028

Christiansen, B. (2007). Atmospheric circulation regimes: Can cluster analysis provide the number? *Journal of Climate*, *20*(10), 2229–2250. https://doi.org/10.1175/JCLI4107.1

Cleveland, W. S., & Devlin, S. J. (1988). Locally weighted regression: An approach to regression analysis by local fitting. *Journal of the American Statistical Association*, *83*(403), 596–610. https://doi.org/10.1080/01621459.1988.10478639

Cortesi, N., González-Reviriego, N., Soret, A., & Doblas-Reyes, F. J. (2017). *Weather regimes: ECMWF seasonal forecasts verification*. (Technical Report). Barcelona Supercomputing Center - Centro Nacional de Supercomputación (BSC-CNS). Retrieved from https://earth.bsc.es/wiki/lib/exe/fetch.php?media=library:external:20170404%7B%5C_%7Dncortesi%7B%5C_%7Dseasonal%7B%5C_%7Dforecasts%7B%5C_%7Dverification.pdf

Cortesi, N., Torralba, V., González-Reviriego, N., Soret, A., & Doblas-Reyes, F. J. (2019). Characterization of European wind speed variability using weather regimes. *Climate Dynamics*, *53*(7–8), 4961–4976. https://doi.org/10.1007/s00382-019-04839-5

Cortesi, N., Torralba, V., Lledó, L., Manrique-Suñén, A., Gonzalez-Reviriego, N., Soret, A., & Doblas-Reyes, F. J. (2021). Yearly evolution of Euro-Atlantic weather regimes and of their sub-seasonal predictability. *Climate Dynamics*, *56*(11–12), 3933–3964. https://doi.org/10.1007/s00382-021-05679-y

D'Andrea, F., Tibaldi, S., Blackburn, M., Boer, G., Déqué, M., Dix, M. R., et al. (1998). Northern Hemisphere atmospheric blocking as simulated by 15 atmospheric general circulation models in the period 1979–1988. *Climate Dynamics*, *14*(6), 385–407. https://doi.org/10.1007/s003820050230

Dawson, A., & Palmer, T. N. (2015). Simulating weather regimes: Impact of model resolution and stochastic parameterization. *Climate Dynamics*, *44*(7), 2177–2193. https://doi.org/10.1007/S00382-014-2238-X

Dawson, A., Palmer, T. N., & Corti, S. (2012). Simulating regime structures in weather and climate prediction models. *Geophysical Research Letters*, *39*(21), 21805. https://doi.org/10.1029/2012GL053284

Doblas-Reyes, F. J., Andreu-Burillo, I., Chikamoto, Y., García-Serrano, J., Guemas, V., Kimoto, M., et al. (2013). Initialized near-term regional climate change prediction. *Nature Communications*, *4*(1), 1715. https://doi.org/10.1038/ncomms2704

Donat, M. G., Leckebusch, G. C., Pinto, J. G., & Ulbrich, U. (2010). European storminess and associated circulation weather types: Future changes deduced from a multi-model ensemble of GCM simulations. *Climate Research*, *42*(1), 27–43. https://doi.org/10.3354/cr00853

Döscher, R., Acosta, M., Alessandri, A., Anthoni, P., Arsouze, T., Bergman, T., et al. (2022). The EC-Earth3 Earth system model for the Coupled Model Intercomparison Project 6. *Geoscientific Model Development*, *15*(7), 2973–3020. https://doi.org/10.5194/GMD-15-2973-2022

Eade, R., Smith, D., Scaife, A., Wallace, E., Dunstone, N., Hermanson, L., & Robinson, N. (2014). Do seasonal-to-decadal climate predictions underestimate the predictability of the real world? *Geophysical Research Letters*, *41*(15), 5620–5628. https://doi.org/10.1002/2014GL061146

EC-Earth. (2019a). EC-Earth-Consortium EC-Earth3 model output prepared for CMIP6 CMIP historical [dataset]. Earth System Grid Federation. https://doi.org/10.22033/ESGF/CMIP6.4700

EC-Earth. (2019b). EC-Earth-Consortium EC-Earth3 model output prepared for CMIP6 DCPP DCPPA-hindcast [dataset]. Earth System Grid Federation. https://doi.org/10.22033/ESGF/CMIP6.4553

Eyring, V., Bony, S., Meehl, G. A., Senior, C. A., Stevens, B., Stouffer, R. J., & Taylor, K. E. (2016). Overview of the Coupled Model Intercomparison Project Phase 6 (CMIP6) experimental design and organization. *Geoscientific Model Development*, *9*(5), 1937–1958. https://doi.org/10.5194/gmd-9-1937-2016

Fabiano, F., Christensen, H. M., Strommen, K., Athanasiadis, P., Baker, A., Schiemann, R., & Corti, S. (2020). Euro-Atlantic weather Regimes in the PRIMAVERA coupled climate simulations: Impact of resolution and mean state biases on model performance. *Climate Dynamics*, *54*(11), 5031–5048. https://doi.org/10.1007/S00382-020-05271-W

Falkena, S. K., de Wiljes, J., Weisheimer, A., & Shepherd, T. G. (2020). Revisiting the identification of wintertime atmospheric circulation regimes in the Euro-Atlantic sector. *Quarterly Journal of the Royal Meteorological Society*, *146*(731), 2801–2814. https://doi.org/10.1002/qj.3818

Fereday, D. R., Knight, J. R., Scaife, A. A., Folland, C. K., & Philipp, A. (2008). Cluster analysis of North Atlantic-European circulation types and links with tropical Pacific sea surface temperatures. *Journal of Climate*, *21*(15), 3687–3703. https://doi.org/10.1175/2007JCLI1875.1

Ferranti, L., Corti, S., & Janousek, M. (2015). Flow-dependent verification of the ECMWF ensemble over the Euro-Atlantic sector. *Quarterly Journal of the Royal Meteorological Society*, *141*(688), 916–924. https://doi.org/10.1002/qj.2411

Fil, C., & Dubus, L. (2005). Winter climate regimes over the North Atlantic and European region in ERA40 reanalysis and DEMETER seasonal hindcasts. *Tellus, Series A: Dynamic Meteorology and Oceanography*, *57*(3), 290–307. https://doi.org/10.1111/j.1600-0870.2005.00127.x

Garrido-Perez, J. M., Ordóñez, C., & García-Herrera, R. (2017). Strong signatures of high-latitude blocks and subtropical ridges in winter PM_{10} over Europe. *Atmospheric Environment*, *167*, 49–60. https://doi.org/10.1016/j.atmosenv.2017.08.004

Giorgetta, M. A., Jungclaus, J., Reick, C. H., Legutke, S., Bader, J., Böttinger, M., et al. (2013). Climate and carbon cycle changes from 1850 to 2100 in MPI-ESM simulations for the Coupled Model Intercomparison Project phase 5. *Journal of Advances in Modeling Earth Systems*, *5*(3), 572–597. https://doi.org/10.1002/JAME.20038

Hagedorn, R., Doblas-Reyes, F. J., & Palmer, T. (2005). The rationale behind the success of multi-model ensembles in seasonal forecasting—I. Basic concept. *Tellus A: Dynamic Meteorology and Oceanography*, *57*(3), 219–233. https://doi.org/10.3402/TELLUSA.V57I3.14657

Hertig, E., & Jacobeit, J. (2014). Variability of weather regimes in the North Atlantic-European area: Past and future. *Atmospheric Science Letters*, *15*(4), 314–320. https://doi.org/10.1002/asl2.505

Japan Meteorological Agency, Japan. (2013). JRA-55: Japanese 55-year reanalysis, daily 3-hourly and 6-hourly data [dataset]. Research Data Archive at the National Center for Atmospheric Research, Computational and Information Systems Laboratory. https://doi.org/10.5065/D6HH6H41

Kageyama, M., D'Andrea, F., Ramstein, G., Valdes, P. J., & Vautard, R. (1999). Weather regimes in past climate atmospheric general circulation model simulations. *Climate Dynamics*, *15*(10), 773–793. https://doi.org/10.1007/S003820050315

Kalnay, E., Kanamitsu, M., Kistler, R., Collins, W., Deaven, D., Gandin, L., et al. (1996). The NCEP/NCAR 40-year reanalysis project. *Bulletin of the American Meteorological Society*, *77*(3), 437–471. https://doi.org/10.1175/1520-0477(1996)077<0437:TNYRP>2.0.CO;2

Kirtman, B., Power, S. B., Adedoyin, A. J., Boer, G. J., Bojariu, R., Camilloni, I., et al. (2013). *Near-term climate change: Projections and predictability*. In *Climate change 2013 the physical science basis: Working Group I Contribution to the Fifth Assessment Report of the Intergovernmental Panel on Climate Change*. https://doi.org/10.1017/CBO9781107415324.023

Kobayashi, S., Ota, Y., Harada, Y., Ebita, A., Moriya, M., Onoda, H., et al. (2015). The JRA-55 reanalysis: General specifications and basic characteristics. *Journal of the Meteorological Society of Japan*, *93*(1), 5–48. https://doi.org/10.2151/jmsj.2015-001

Kushnir, Y., Scaife, A. A., Arritt, R., Balsamo, G., Boer, G., Doblas-Reyes, F., et al. (2019). Towards operational predictions of the near-term climate. *Nature Climate Change*, *9*(2), 94–101. https://doi.org/10.1038/s41558-018-0359-7

Mariotti, A., Baggett, C., Barnes, E. A., Becker, E., Butler, A., Collins, D. C., et al. (2020). Windows of opportunity for skillful forecasts subseasonal to seasonal and beyond. *Bulletin of the American Meteorological Society*, *101*(5), E608–E625. https://doi.org/10.1175/BAMS-D-18-0326.1

Masato, G., Hoskins, B. J., & Woollings, T. (2013). Winter and summer Northern Hemisphere blocking in CMIP5 models. *Journal of Climate*, *26*(18), 7044–7059. https://doi.org/10.1175/JCLI-D-12-00466.1

Meehl, G. A., Goddard, L., Murphy, J., Stouffer, R. J., Boer, G., Danabasoglu, G., et al. (2009). Decadal prediction. *Bulletin of the American Meteorological Society*, *90*(10), 1467–1486. https://doi.org/10.1175/2009bams2778.1

Meehl, G. A., Richter, J. H., Teng, H., Capotondi, A., Cobb, K., Doblas-Reyes, F., et al. (2021). Initialized Earth system prediction from subseasonal to decadal timescales. *Nature Reviews Earth & Environment*, *2*(5), 340–357. https://doi.org/10.1038/s43017-021-00155-x

Merryfield, W. J., Baehr, J., Batté, L., Becker, E. J., Butler, A. H., Coelho, C. A., et al. (2020). Current and emerging developments in subseasonal to decadal prediction. *Bulletin of the American Meteorological Society*, *101*(6), E869–E896. https://doi.org/10.1175/BAMS-D-19-0037.1

Michelangeli, P.-A., Vautard, R., & Legras, B. (1995). Weather regimes: Recurrence and quasi stationarity. *Journal of the Atmospheric Sciences*, *52*(8), 1237–1256. https://doi.org/10.1175/1520-0469(1995)052<1237:WRRAQS>2.0.CO;2

Molteni, F., Stockdale, T., Balmaseda, M., Balsamo, G., Buizza, R., Ferranti, L., et al. (2011). The new ECMWF seasonal forecast system (System 4). *ECMWF technical report*.

National Centers for Environmental Prediction, National Weather Service, NOAA, & U.S. Department of Commerce. (1994). NCEP/NCAR global reanalysis products, 1948-continuing [dataset]. Research Data Archive at the National Center for Atmospheric Research, Computational and Information Systems Laboratory. Retrieved from https://rda.ucar.edu/datasets/ds090.0/

Ordóñez, C., Barriopedro, D., Garciá-Herrera, R., Sousa, P. M., & Schnell, J. L. (2017). Regional responses of surface ozone in Europe to the location of high-latitude blocks and subtropical ridges. *Atmospheric Chemistry and Physics*, *17*(4), 3111–3131. https://doi.org/10.5194/acp-17-3111-2017

Pérez-Zanón, N., Caron, L.-P., Terzago, S., Schaeybroeck, B. V., Lledó, L., Manubens, N., et al. (2021). The CSTools (v4.0) toolbox: From climate forecasts to climate forecast information. *Geoscientific Model Development Discussions*, *2021*, 1–32. https://doi.org/10.5194/gmd-2021-368

Philipp, A., Bartholy, J., Beck, C., Erpicum, M., Esteban, P., Fettweis, X., et al. (2010). Cost733cat – A database of weather and circulation type classifications. *Physics and Chemistry of the Earth*, *35*(9–12), 360–373. https://doi.org/10.1016/j.pce.2009.12.010

Rodwell, M. J., Rowell, D. P., & Folland, C. K. (1999). Oceanic forcing of the wintertime North Atlantic Oscillation and European climate. *Nature*, *398*(6725), 320–323. https://doi.org/10.1038/18648

Scaife, A. A., & Smith, D. (2018). A signal-to-noise paradox in climate science. *npj Climate and Atmospheric Science*, *1*, 28. https://doi.org/10.1038/s41612-018-0038-4

Schiemann, R., Demory, M. E., Shaffrey, L. C., Strachana, J., Vidale, P. L., Mizielinski, M. S., et al. (2017). The resolution sensitivity of Northern Hemisphere blocking in four 25-km atmospheric global circulation models. *Journal of Climate*, *30*(1), 337–358. https://doi.org/10.1175/JCLI-D-16-0100.1

Smith, D. M., Eade, R., Scaife, A. A., Caron, L. P., Danabasoglu, G., DelSole, T. M., et al. (2019). Robust skill of decadal climate predictions. *npj Climate and Atmospheric Science*, *2*(1), 13. https://doi.org/10.1038/s41612-019-0071-y

Smith, D. M., Scaife, A. A., Eade, R., Athanasiadis, P., Bellucci, A., Bethke, I., et al. (2020). North Atlantic climate far more predictable than models imply. *Nature*, *583*(7818), 796–800. https://doi.org/10.1038/s41586-020-2525-0

Stephenson, D. B., Hannachi, A., & O'Neill, A. (2004). On the existence of multiple climate regimes. *Quarterly Journal of the Royal Meteorological Society*, *130*(597), 583–605. https://doi.org/10.1256/QJ.02.146

Stryhal, J., & Huth, R. (2017). Classifications of winter Euro-Atlantic circulation patterns: An intercomparison of five atmospheric reanalyses. *Journal of Climate*, *30*(19), 7847–7861. https://doi.org/10.1175/JCLI-D-17-0059.1

Sutton, R. T., & Allen, M. R. (1997). Decadal predictability of North Atlantic sea surface temperature and climate. *Nature*, *388*(6642), 563–567. https://doi.org/10.1038/41523

Torralba, V. (2019). *Seasonal climate prediction for the wind energy sector: Methods and tools for the development of a climate service* (Doctoral dissertation). Complutense University of Madrid.

Torralba, V., Gonzalez-Reviriego, N., Cortesi, N., Manrique-Suñén, A., Lledó, L., Marcos, R., et al. (2021). Challenges in the selection of atmospheric circulation patterns for the wind energy sector. *International Journal of Climatology*, *41*(3), 1525–1541. https://doi.org/10.1002/joc.6881

Walz, M. A., Donat, M. G., & Leckebusch, G. C. (2018). Large-scale drivers and seasonal predictability of extreme wind speeds over the North Atlantic and Europe. *Journal of Geophysical Research: Atmospheres*, *123*(20), 11518–11535. https://doi.org/10.1029/2017JD027958

Wilks, D. S. (2011). Forecast verification. *International Geophysics*, *100*, 301–394. https://doi.org/10.1016/B978-0-12-385022-5.00008-7

Yeager, S. G., Danabasoglu, G., Rosenbloom, N. A., Strand, W., Bates, S. C., Meehl, G. A., et al. (2018). Predicting near-term changes in the Earth system: A large ensemble of initialized decadal prediction simulations using the Community Earth System Model. *Bulletin of the American Meteorological Society*, *99*(9), 1867–1886. https://doi.org/10.1175/BAMS-D-17-0098.1

Zwiers, F. W., & von Storch, H. (1995). Taking serial correlation into account in tests of the mean. *Journal of Climate*, *8*(2), 336–351. https://doi.org/10.1175/1520-0442(1995)008<0336:TSCIAI>2.0.CO;2